NANO · MICRO small
www.small-journal.com

A Photoorganizable Triple Shape Memory Polymer for Deployable Devices

Jiahao Sun, Bo Peng, Yao Lu, Xiao Zhang, Jia Wei, Chongyu Zhu, and Yanlei Yu*

Inspired by the action and healing process from living organisms, developing deployable devices using stimuli-responsive materials, or "smart" deployable devices, is desired to realize remote-controlled programmable deformation with additional in situ repair to perform multiple tasks while extending their service life in aerospace. In this work, a photoorganizable triple shape memory polymer (POTSMP) is reported, which is composed of an azobenzene-containing thermoplastic polyurethane. Upon UV and visible illumination, this POTSMP performs arbitrary programming of two temporary shapes and precise and stepwise shape recovery, exhibiting various temporary shapes adapted to different aerospace applications. On the other hand, rapid light-reconfiguration in seconds, including light-reshaping and light-welding, is achieved in response to UV irradiation, allowing in situ localized process and repair of permanent shape. Combining these photoorganizable operations, deformable devices with complex 2D/3D structures are facilely manufactured with no need of special molds. It is envisioned that this POTSMP can expand the potential of photoresponsive TSMPs in smart deployable devices.

1. Introduction

Deployable structures have been widely used in the aviation field to construct foldable solar panels, collapsible reflector antennas, and expandable space habitats.[1,2] These devices occupy minimal space during transportation, while converting into complex structures controlled by electric motors when in use. Recently, a conceptual design of "smart" deployable devices using shape memory polymers (SMPs) has been proposed to further reduce the weight of aviation equipment and simplify their operation.[3] SMPs provide programmable deformation from temporary shapes (TS, controlled by switching domains) to original permanent shapes (PS, fixed by netpoints) upon suitable stimuli. In comparison to other light weighted smart materials such as dielectric elastomers, hydrogels, or liquid crystal elastomers,[4–8] SMPs offer a high degree of freedom in shape programming and the ability to maintain shape without continuous energy input, meeting the need of "smart" deployable devices to deform between multiple functional shapes in sequence and provide the corresponding functionality needs.[9–11] Compared to dual-SMPs with single shape deformation,[12–17] triple shape memory polymers (TSMPs) produce additional temporary shape so that they are compatible to different programming pathways and stepwise shape deformation among more intermediate shapes,[18–22] permitting "smart" deployable devices to complete multiple tasks accordingly.

Taking advantage of light as a remote stimulus that propagates directionally, photoresponsive SMPs are more energy efficient and offer control with high spatiotemporal resolution, beneficial for outer space applications.[15,23–27] With the aid of photothermal conversion particles/dyes or photoreactive groups, people have investigated TSMPs with two light-controlled switching domains for remote shape deformation control.[28–32] To realize arbitrary programming and recovering to two temporary shapes by light, the two switching domains should be individually triggered by different light conditions.[9,33,34] Thus, the molecular design of these photoresponsive TSMPs is rather difficult and often involves complicate synthesis.[29,30] Recently, Zhao et al. developed a photothermal-driven TSMP using an azobenzene-containing polymer with two thermoresponsive switching domains.[31] By adjusting the intensity of the irradiated UV, they succeeded in tuning the photothermal effect of azobenzene dye, inducing the localized and stepwise deformations of two TSs.

Besides the enrichment of TSs, PS with high structural complexity is also crucial for SMPs to obtain specific functions for versatile deployable aerospace devices.[35–38] Different from nonresponsive chemical crosslinking netpoints,[29] the construction of stimuli-reversible netpoints in TSMPs supplies the reconfiguration of their PSs into delicate 2D/3D structures after manufacture.[39–42] For example, by introducing thermoresponsive dynamic covalent bonds as netpoints into an azobenzene-containing polymer, Kessler et al. demonstrated a photothermal-driven TSMPs with reconfigurable permanent shapes, through which they acquired a 3D PS from a flat sheet by simple thermal treatment.[32] They also suggested the light reconfiguration of PS was possible by tuning these dynamic netpoints by the photothermal effect of azobenzene units. Although a slow reconfiguration process (about several hours)

J. Sun, B. Peng, Y. Lu, X. Zhang, J. Wei, C. Zhu, Y. Yu
Department of Materials Science and State Key Laboratory of Molecular Engineering of Polymers
Fudan University
Shanghai 200433, China
E-mail: cy_zhu@fudan.edu.cn

The ORCID identification number(s) for the author(s) of this article can be found under https://doi.org/10.1002/smll.202106443.

DOI: 10.1002/smll.202106443

and compromising mechanical property was resulted in their case, it is foreseeable that TSMPs with both the light-controlled netpoints and switching domains, which we define as photo-organizable TSMPs to distinguish with these TSMPs containing only light-controlled switching domains, are promising candidates as the "smart" deployable devices that are (re)configurable or repairable at work.

Herein, we report a photoorganizable TSMP (POTSMP) with rapid response by the careful molecular design of the light-controlled switching domains and netpoints in an azobenzene-containing thermoplastic polyurethane (**Figure 1**a,b). By switching the wavelength and intensity of light, we manage to trigger different photoresponsive mechanisms of azobenzene units, granting POTSMP to perform fast shape (re)configuration of PS with stepwise shape programming and recovery of two TSs (Figure 1c,d). With all these photoorganizable operations, we demonstrate the potential of POTSMP to build deformable antenna mounts and deployable aerospace base for aviation applications.

2. Result and Discussion

2.1. Design and Preparation

To acquire such a POTSMP, azobenzene-containing polymer is chosen as its unique photoresponse. Apart from harvesting photothermal energy as a UV-absorbing dye,[28,31,32] it has been known that the azobenzene moieties in azobenzene-containing polymers undergo reversible *trans-cis* photoisomerization and disturb the polymer chain segments in response to UV and visible light.[43] Such photochemical effect has not only been widely applied in liquid crystal polymers to perform the bending toward or back to the light source,[44] this mechanism also regulates the polymer T_g (as known as the photoswitchable T_g effect)[45] and has applied to control the switching domain in a dual-SMP to realize the athermal temporary shape programming and recovery.[24] Combining this mechanism with photothermal effect, we may use azobenzene units as the only trigger to independently program and recovery from two temporary shapes in an athermal and photothermal manner by light, leading to a facile synthesis and simpler operation condition.

Additionally, the introduction of photoswitchable T_g effect also gives opportunity to balance the trade-off between the processibility and stability of PS. Typically, a temperature gap is essential for the independent control of two photothermal-responsive switching domains in conventional photothermal-driven TSMPs.[31] Therefore, chemical crosslinking netpoints are needed to avoid the potential heat-induced creep during shape memory operation.[33,34] By controlling the two switching domains via two different photoresponsive mechanisms, a much lower overall operating temperature will be resulted for stepwise shape deformation. Hence, in contrast to chemical

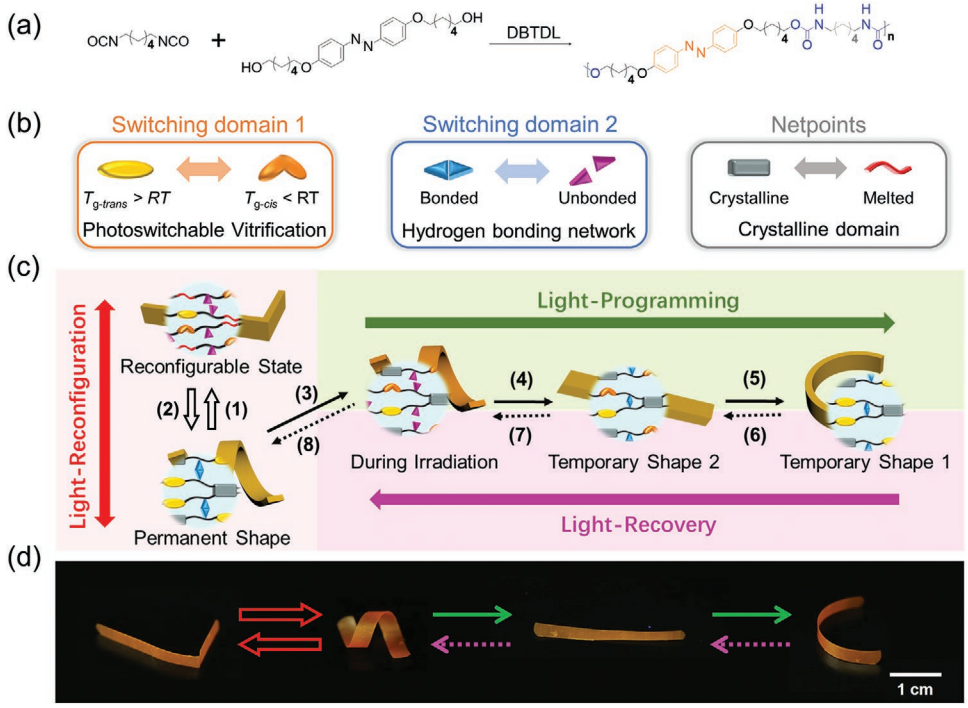

Figure 1. Design and deformation mechanism of POTSMP. a) Synthetic route for POTSMP. The main components to realize triple shape memory are highlighted. b) Diagram of switching domains and netpoints of POTSMP before and after response. c) Schematic showing the full-light-controlled permanent shape reconfiguration, light-programming, and light-recovery process of POTSMP. The flow of the reconfiguration process (steps 1–2) is indicated by the hollow arrows, while the programming process (steps 3–5) is guided by solid arrows and the recovery process (steps 6–8) is indicated by dashed arrows. Step conditions: 1) 500 mW cm^{-2} UV (365 nm) illumination for 15 s; 2) cooling down under stress and 80 mW cm^{-2} visible (530 nm) illumination for 60 s; 3) 150 mW cm^{-2} UV (365 nm) illumination for 15 s; 4) cooling down under stress; 5) 80 mW cm^{-2} visible (530 nm) illumination under stress for 60 s; 6) 50 mW cm^{-2} UV (365 nm) illumination for 300 s; 7) 150 mW cm^{-2} UV (365 nm) illumination for 15 s; 8) cooling down and 80 mW cm^{-2} visible (530 nm) illumination for 60 s. d) Physical diagram of each stage of the light-organization process of POTSMP.

crosslinking, crystalline domains are applicable as the physical crosslinking netpoints, which enables more rapid reconfiguration of permanent shape through the melting and recrystallizing process (typically within seconds) by photothermal effect.[46]

According to this concept, an azobenzene-containing thermoplastic polyurethane is designed as POTSMP (Figure 1a). As demonstrated in Figure 1b,c, the vitrification of this azobenzene-containing polymer is set as a switching domain (SD1) to control the temporary shape 1 (TS1) by applying the photoswitchable T_g effect. The hydrogen bonding network formed by urethane bonds, on the other hand, is designed to serve as switching domain (SD2) to control the temporary shape 2 (TS2) in response to photothermal effect. Owing to the linear polymer structure as well as the presence of hydrogen bonding network, crystalline domains with high transition temperature will be obtained, acting as reconfigurable netpoints to fix PS.

Through a two-step reaction (Figure 1a and Figures S1 and S2, Supporting Information), a photoresponsive monomer (BH6AB) is first synthesized from a commercially available azobenzene derivative via Williamson reaction, and then react with hexamethylene diisocyanate by polyaddition to produce POTSMP. POTSMP possesses stable crystalline domains (T_m ~ 170 °C), constructing the netpoints as desired. Its glass transition temperature (T_g ~ 61.8 °C) is above room temperature, which is crucial for the light-induced regulation of SD1 (Figure S3, Supporting Information). Fourier transform infrared spectroscopy (FT-IR) reveals that the signal of hydrogen bonded urethane C=O group (1690 cm^{-1}) is much intense than the free ones (1720 cm^{-1}), indicating a strong hydrogen bonding network is presented in POTSMP as SD2 (Figure S4, Supporting Information).

2.2. Photoorganizable Operations of POTSMP

Compared to the previously reported photoresponsive TSMPs containing chemical crosslinking netpoints, POTSMP with physical crosslinking netpoints is soluble and moldable so that it is compatible to more processing techniques, including solution processing, melt spinning, molding, etc., for the construction and reconfiguration of its PS (Figure S5, Supporting Information). Furthermore, since the temperature of POTSMP can be elevated through photothermal effect by UV light, the local processing of POTSMP (light reconfiguration) becomes feasible (Figure 1d, indicating by red arrows), which is one key process for photoorganizable operations. As shown in **Figure 2**a, the temperature of illuminated POTSMP was linearly dependent to the intensity of UV light and reached 200 °C ($>T_m$) in 10 s upon 500 mW cm^{-2} UV irradiation. Such temperature is enough to rapidly melt the crystalline domains in POTSMP. Meanwhile, the high decomposition temperature ($T_{5\%}$ ~ 350 °C) of POTSMP (Figure S6, Supporting Information) guarantees its repeatable processing and recycling without changing its chemical and physical properties.

Applying localized illumination to melt (Figure 1c, step 1) and reconstruct (Figure 1c, step 2) the crystalline domains, various PSs with complex 2D/3D structures were manufactured through the light-reconfiguration process, including reshaping single sample (light-reshaping) and jointing multiple samples together (light-welding) (Figure 2b). The reconfigured structure exhibited similar mechanical properties to those obtaining from thermal treatment (Figures S7 and S8, Supporting Information), giving a better performance than the photoresponsive TSMP using dynamic covalent bonds as netpoints. Moreover, the light reconfiguration was accelerated hundreds of times in our case, which completed within 20 s, favoring for the rapid construction and repair of "smart" deployable devices with complex structures in outer space.

In addition, excellent light-induced triple shape memory performance is essential for POTSMP, where the key is to individually manipulate the two temporary shapes (TS1 & TS2) by two photoresponse mechanisms. As shown in Figure 2d,e and Figure S9, Supporting Information, the ratio of azobenzene isomers in POTSMP is adjustable upon UV and visible illumination, which affects the T_g of POTSMP same as other azobenzene-containing polymers. The T_g of unilluminated photoorganizable TSMP reduced from 61.8 °C (*trans*-form, the yellow sample) to −10.7 °C (*cis*-form, the red sample) after UV irradiation, while recovered after visible light irradiation (530 nm). Hence, we may place POTSMP between glassy state and rubbery state by UV and visible light, allowing the light manipulation of its TS1 at ambient temperature. On the other side, consistent to literature,[47] the hydrogen bonding network formed by the urethane bonds in POTSMP reversibly dissociated and reassociated with the increase and reduction of temperature (Figure 2c and Figure S10, Supporting Information), indicating the ratio of bonded and unbonded urethane groups is tunable for the subsequent programming and recovery process of TS2 by photothermal effect.

Combining abovementioned photothermal and photochemical effects, the light programming and light recovery of POTSMP were realized by simply adjusting the light source (Figure 1d). During the light programming (Figure 1c, steps 3–5), two temporary shapes of POTSMP were separately programmed through sequential irradiation of UV light (365 nm, 150 mW cm^{-2}) and visible light (530 nm, 80 mW cm^{-2}). Upon UV irradiation, POTSMP underwent photoswitchable T_g effect, reducing its T_g below room temperature while the photothermal effect heated up the polymer to dissociate the hydrogen bonding network (Figure 1c, step 3). At this point, SD1 and SD2 were activated simultaneously. After programming TS2, the UV source was removed and POTSMP cooled to room temperature, allowing the reassociation of hydrogen bonding network to fix TS2 (Figure 1c, step 4). Meanwhile, the ratio of *cis*-form azobenzene units in POTSMP remained unchanged (**Figure 3**a) so that POTSMP stayed in the rubbery state, enabling the programming of TS1. Once the desired TS1 was obtained, visible light was irradiated onto POTSMP to recover the T_g back above room temperature and POTSMP turned back to the glassy state to fix TS1 (Figure 1c, step 5). The stepwise light-recovery process (Figure 1c, steps 6–8), on the other hand, was completed by adjusting UV light intensity (Movie S1, Supporting Information). Upon irradiation of 50 mW cm^{-2} UV light, POTSMP at TS1 went into rubbery state due to the photoswitchable T_g effect without generating significant heat, and recovered to TS2 (Figure 1c, step 6). Once the UV intensity was increased to 150 mW cm^{-2}, the hydrogen bonding network in POTSMP

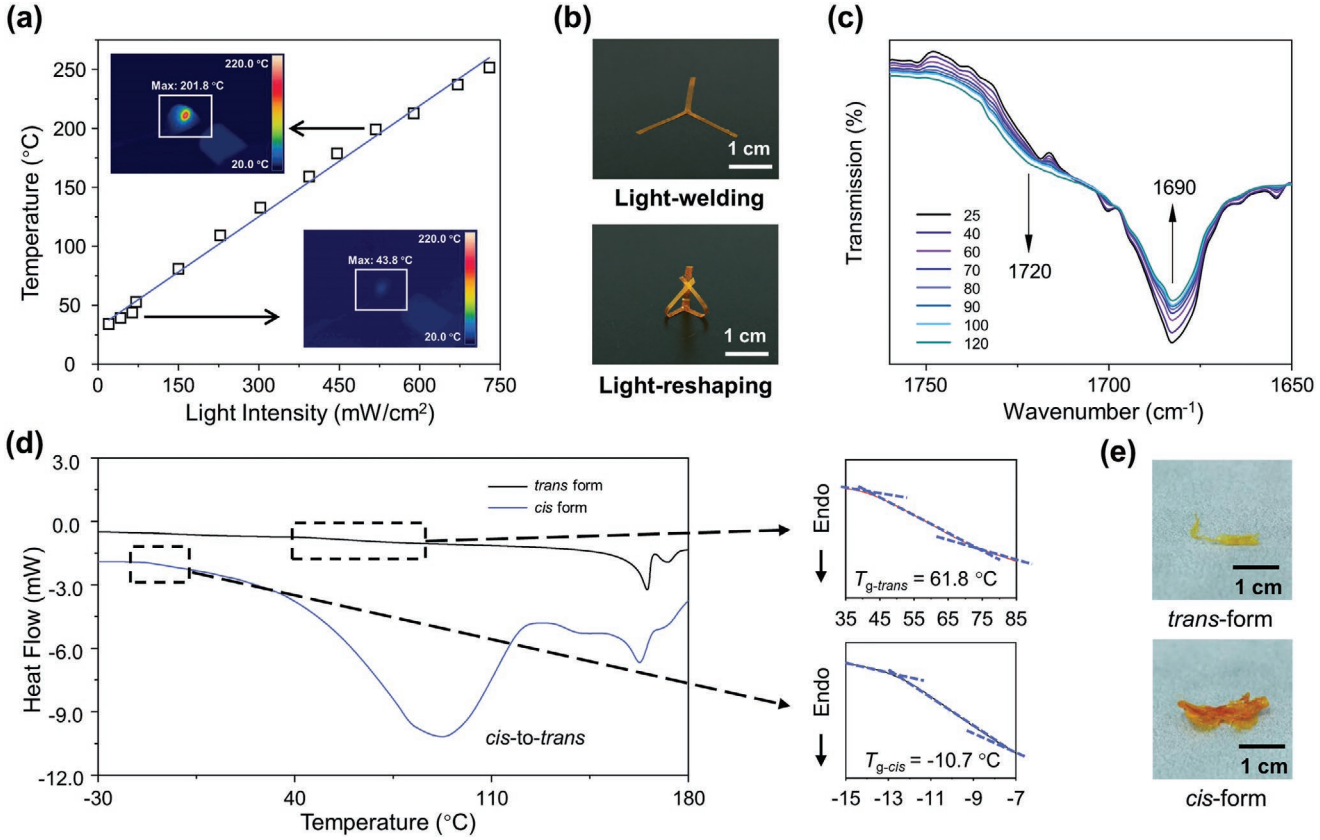

Figure 2. Light-controlled triple shape memory property of POTSMP. a) Photothermal effect of POTSMP after 15 s irradiation of 365 nm UV light at different intensities. IR thermal imaging suggests the photothermal effect of POTSMP is negligible under 64 mW cm^{-2} UV illumination (lower right picture) while the temperature of POTSMP reaches 200 °C under 518 mW cm^{-2} UV illumination (upper left picture). b) 2D/3D permanent shapes of POTSMP after light-reconfiguration through photothermal effect. c) The zoom-in FT-IR of POTSMP at different temperatures. The signal of the hydrogen bonded urethane C=O groups with N—H group (1690 cm^{-1}) decreases and the signal of free urethane C=O groups (1720 cm^{-1}) increases with the elevation of temperature, indicating the hydrogen bonding network gradually dissociated with the increase of the temperature. d) The DSC heating curves of *trans*-form and *cis*-form POTSMP. The T_g of *trans*-form and *cis*-form POTSMP are shown in the zoomed-in data. e) Images of *trans*-form and *cis*-form POTSMP. The orange color of *cis*-form POTSMP indicates the high *cis* ratio of azobenzene units. The thickness of the two samples was about 10 µm. The color of both samples will deepen with the increase of thickness (i.e., *trans*-form POTSMP appears orange color while *cis*-form POTSMP shows red color at the thickness of 110 µm).

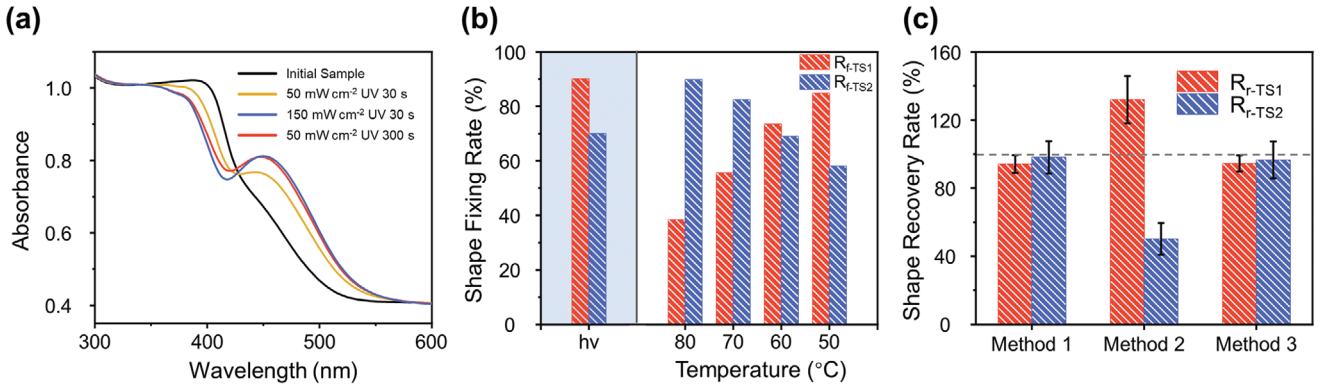

Figure 3. a) UV-vis absorption spectra of POTSMP after being irradiated with 50 and 150 mW cm^{-2}, 365 nm UV light. The data indicate the ratio of *cis*-form azobenzene was not affected by photothermal effect, which is crucial to realize high fixing rates during light programming. b) The shape fixing rates of POTSMP through light programming and thermal programming tested by a bending method. In the light-programming process, 365 nm UV (150 mW cm^{-2}) was used for programming of TS2 and TS1 was programmed by 365 nm UV (50 mW cm^{-2}). In the thermal-programming process, the programming of TS2 was performed at 90 °C, while the programming of TS1 was performed at 50, 60, 70, and 80 °C, respectively (film thickness: 110 µm). c) A comparison of triple shape recovery of a light-programmed POTSMP by different methods. Method 1: TS2 and TS1 were both recovered by 365 nm UV light stimulation (50 and 150 mW cm^{-2}). Method 2: TS2 and TS1 were both recovered by thermal stimulation (60 and 90 °C). Method 3: TS1 was recovered by 365 nm UV light (50 mW cm^{-2}) first and then TS2 was recovered by thermal treatment (90 °C) (film thickness: 110 µm).

was dissociated due to photothermal effect, and POTSMP was recovered to its PS (Figure 1c, steps 7–8).

It is worth noting that, owing to the unique structure of POTSMP, the *cis*-form POTSMP appeared a more stable conformation than the *trans*-form POTSMP, confirming by the endothermic peak rather than a previously reported exothermic peak[20] around 90 °C on the first differential scanning calorimetry (DSC) cycle of the *cis*-form POTSMP (Figure 2d). This suggests that the thermal stability of the *cis*-state azobenzene units is enhanced by the polymer backbone and hydrogen bonding network in POTSMP. Unlike thermoplastic azobenzene polymers without hydrogen bonding network (Figure S11, Supporting Information), the azobenzene unit in POTSMP maintains a high *cis* state ratio throughout the light programming of TS2 despite the photothermal action of UV light as shown in Figure 3a, demonstrating that SD1 is not involved in the programming of TS2. Hence, the light programming of TS1 and TS2 can be separately controlled through two individually controlled mechanisms, guaranteeing a high shape fixing rate for both temporary shapes.

To quantify the shape memory of POTSMP, a further investigation on its shape fixing rate and recovery rate was conducted using a bending method adapted from previous report.[24,48] Since the two switching domains in POTSMP were also responsive to heat, both light-induced and thermal-induced shape fixing rates and recovery rates were tested. As shown in Figure 3b, the fixing rate of two temporary shapes in the thermal-controlled process is a trade-off, and only one temporary shape can obtain a high fixing rate at the same time, while in the light-controlled process, two temporary shapes ($R_{f\text{-}TS2}$ > 90%, $R_{f\text{-}TS1}$ > 70%, shown in Figures S12 and S13, Supporting Information) can both obtain a relatively high shape fixing rate at the same time. Therefore, on balance, the light-controlled shape fixing rate is better than the thermal-controlled one at any test temperature. This is due to that the glass transition (≈50 to 80 °C) and hydrogen bond dissociation (>RT) of POTSMP overlap during the thermal programming process (Figure S14, Supporting Information). In the temperature range from 50 to 80 °C, the overlapping parts of the two switching domains can only be activated or frozen at the same time. In contrast, the two switching domains are controlled separately by two light-controlled mechanisms during the light-programming process. When the light-programmed TS2 was fixed by the hydrogen bonding network through photothermal effect, azobenzene units remained in *cis* form so that POTSMP maintained the rubbery state. Therefore, the entropy energy variation of TS2 was fully stored through the hydrogen bonding network and the entropy energy change of TS1 was preserved by the vitrification of chain segments, preventing the unwanted entropy energy release during shape programming, thereby obtaining a high shape fixing rate.

Furthermore, the light-induced and thermal-induced shape recovery rates were measured. Since the photoswitchable T_g effect and photothermal effect during the light programming are insufficient to disrupt the crystalline domains (netpoints), the topological network of PS is well retained. Therefore, POTSMP after light programming exhibited excellent light-recovery rates exceeded 90% in both shape recovery processes (Figure 3c, Method 1). Meanwhile, the same material presented a shape recovery rate ($R_{r\text{-}TS1}$ ~ 132%) more than 100% during thermally induced shape recovery from TS1 to TS2 and a shape recovery rate ($R_{r\text{-}TS2}$ ~ 50%) less than 50% during TS2 to PS, owing to the overlapped responsive temperatures of two switching domains (Figure 3c, Method 2). Once the shape recovery from TS1 to TS2 was conducted upon UV illumination to separately activate SD1, the thermal-induced shape recovery of TS2 to PS produces similar recovery rate as the one from light-induced photothermal effect (Figure 3c, Method 3).

As discussed above, the combination of the photothermal effect with the photoswitchable T_g effect allows both switching domains to function independently at lower temperatures. It ensures crystalline domains as netpoints to simultaneously provide good processibility and high shape memory performance, laying a solid foundation to conduct the photoorganizable operations.

2.3. Light-Controlled Processing and Deformation of Structural Component Promising for Aerospace Applications

In aerospace application, antennas are usually foldable to save space at launch and are assembled into different preset shapes by motor-driven stands to transmit signals with different radiation characteristics. Benefiting from the remote and precise control of light stimulation, new "intermediate" temporary shapes from the pre-programming TSs are enriched by localized light recovery, promising the preparation of shape-shifting antennas with multiple radiative properties.

To illustrate this, a demo of "smart" antenna is presented using POTSMP as shown in **Figure 4**a. A POTSMP sample was light-reconfigured into an "O" shape (PS), and then light-programmed into an "I" shape (TS2) and a "W" shape (TS1). In traditional thermal-controlled shape recovery process, the sample deformed as a whole and produced only three preset shapes "W," "I," "O" with compromising shape recovery rates (Figure 4b). In comparison, the light-recovery process realizes the localized shape recovery triggered by photothermal and/or photochemical effects. Through the localized light recovery, the sample recovers to its TS1 or PS only at the illuminated part, while the rest part remains in TS2 or TS1, producing a mixed TS1/TS2 or TS2/PS in one sample to give additional "intermediate" TSs. As shown in Figure 4c, by irradiating the positions indicated by the arrows, the stand demo achieves a localized shape recovery process and recovered from "W" to "V," "I," "U," "C," and "O" in sequence. This programmed and localized light-recovery process shows that the light-controlled TSMP far exceeds the shape manipulation capability of the thermal recovery process, providing more control opportunities for the morphological regulation of shape memory antenna stands.

In addition, the photoorganizable operations allow POTSMP to perform shape reconfiguration during deformation, offering a much simpler processing strategy for fabricating deployable devices. With the aid of programmed shape deformations and reconfigurations during the deployment process, complex self-standing 3D structure can be generated from a flat polymer sheet without customized mold. As shown in **Figure 5**, we demonstrate the production of a kirigami 3D space capsule

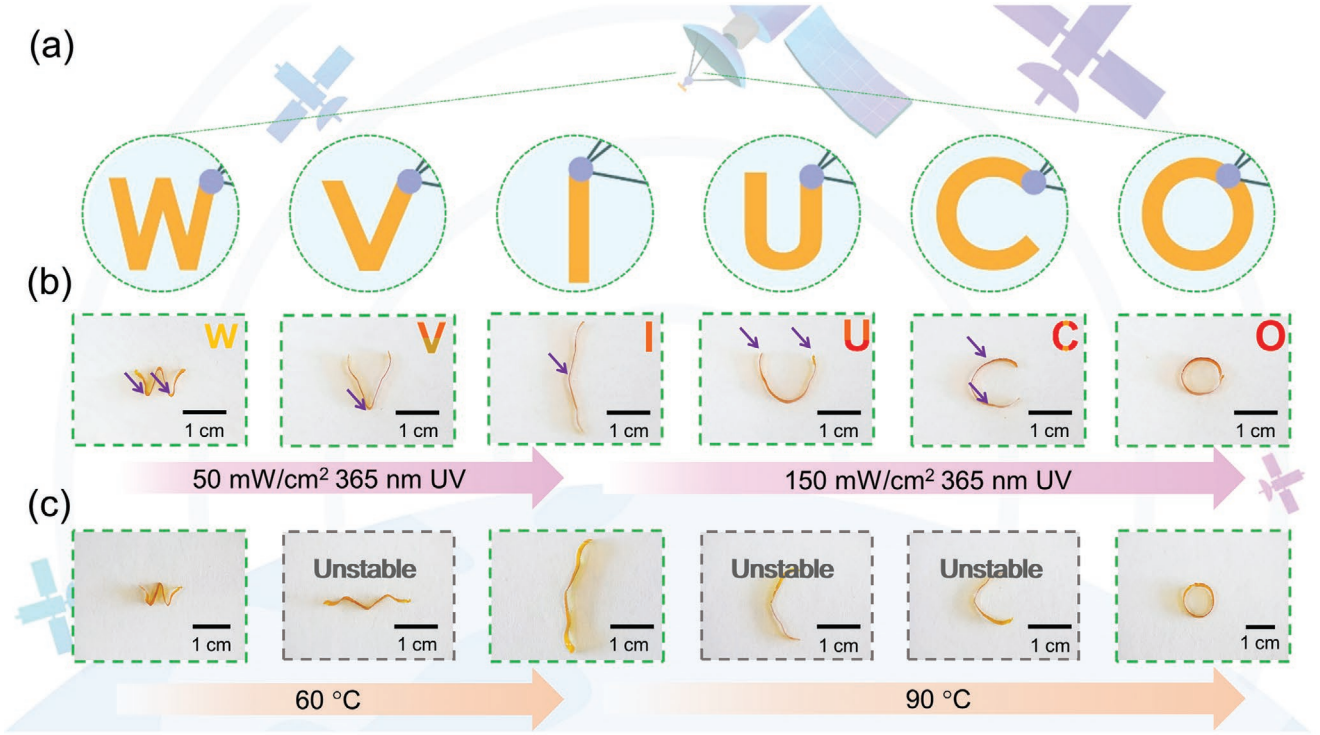

Figure 4. Comparison between localized light recovery and overall heat treatment of a demo of "smart" antenna to produce additional temporary shapes at mixed TS1/TS2 or TS2/PS states. a) Schematic diagram of different shapes of a "smart" antenna. b) The light-recovery process of the demo of "smart" antenna. The sample was irradiated by 365 nm UV light (50 or 150 mW cm^{-2}) at the position pointed by the arrows in sequence, producing the letter "W" (TS1), "I" (TS2), "O" (PS) and three additional temporary shapes at mixed TS1/TS2 or TS2/PS states (letter "V," "U," and "C"). In the schematic diagram in the upper right corner of each image, the PS, TS2, and TS1 part of the sample is marked in red, orange, and yellow, respectively. c) The shape recovery of the demo of "smart" antenna by overall heating on a hot stage at 60 and 90 °C. The sample only produced three predetermined letter "W" (TS1) and "I" (TS2) and "O" (PS).

frame model through photoorganizable operations, presenting a demo for the storage–transportation–reassembly process of a space capsule frame. The 3D initial PS was folded from a flat POTSMP sheet in a few seconds through localized light reshaping. A curled transporting shape (TS2) and a flat storage shape (TS1) with grooves were then light programmed in sequence for subsequent deformation and saved space during storage and transportation. After reaching the target place, the flat storage state (TS1) was first cut into TS1' (shown in Figure S15, Supporting Information) to ensure the further designed kirigami deformation. Then TS1' was recovered to the curled transporting shape upon UV illumination (50 mW cm^{-2}) to reduce the width and pass through the transport barn door. As light-reconfiguration process of PS possessed high spatial resolution, a closed tubular structure (TS2') was further processed in 10 s through the localized light-welding process without releasing the entropy energy stored in the unilluminated parts, showing superiority to the conventional thermal treatment. Finally, upon UV illumination (150 mW cm^{-2}), the tubular TS2' underwent second light recovery, producing the targeted 3D space capsule frame (new PS) with more complex 3D structure rather than the initial PS due to the in situ processed cutout and light welding during the light-recovery process. Our design gives opportunity to process complex aerospace structures that are lightweight, expandable, and can be assembled quickly.

3. Conclusion

In summary, we present a POTSMP, including PS (re)configuration, two temporary shape programming, and recovery process. Applying the photoswitchable T_g effect and the photothermal-induced hydrogen bonding network dissociation, two programmable TSs are controlled separately by the facile manipulation of light to give stepwise and precise deformation. Moreover, the precise and rapid photoorganizable operations provide a new shape processing strategy, which enables the facile processing of complex 2D/3D structures. Through light as a remote and precise stimulus, both the permanent shape and the temporary shape of the POTSMP are controlled with high spatiotemporal resolution, providing a material basis for the design of a single actuator integrating multiple functions for complicated tasks. With a further improvement of the strength and stability of POTSMP, we believe it can act as a promising alternative to the current metal-based deployable devices for low or no-gravity cosmic environments. Jointing this material with advanced processing techniques such as additive manufacturing, it is anticipated to realize the photoorganizable operation in more complex and large-scale devices.

4. Experimental Section

Preparation of POTSMP with a Permanent Shape by Light Reconfiguration: The POTSMP powder was first hot-pressed at 220 °C,

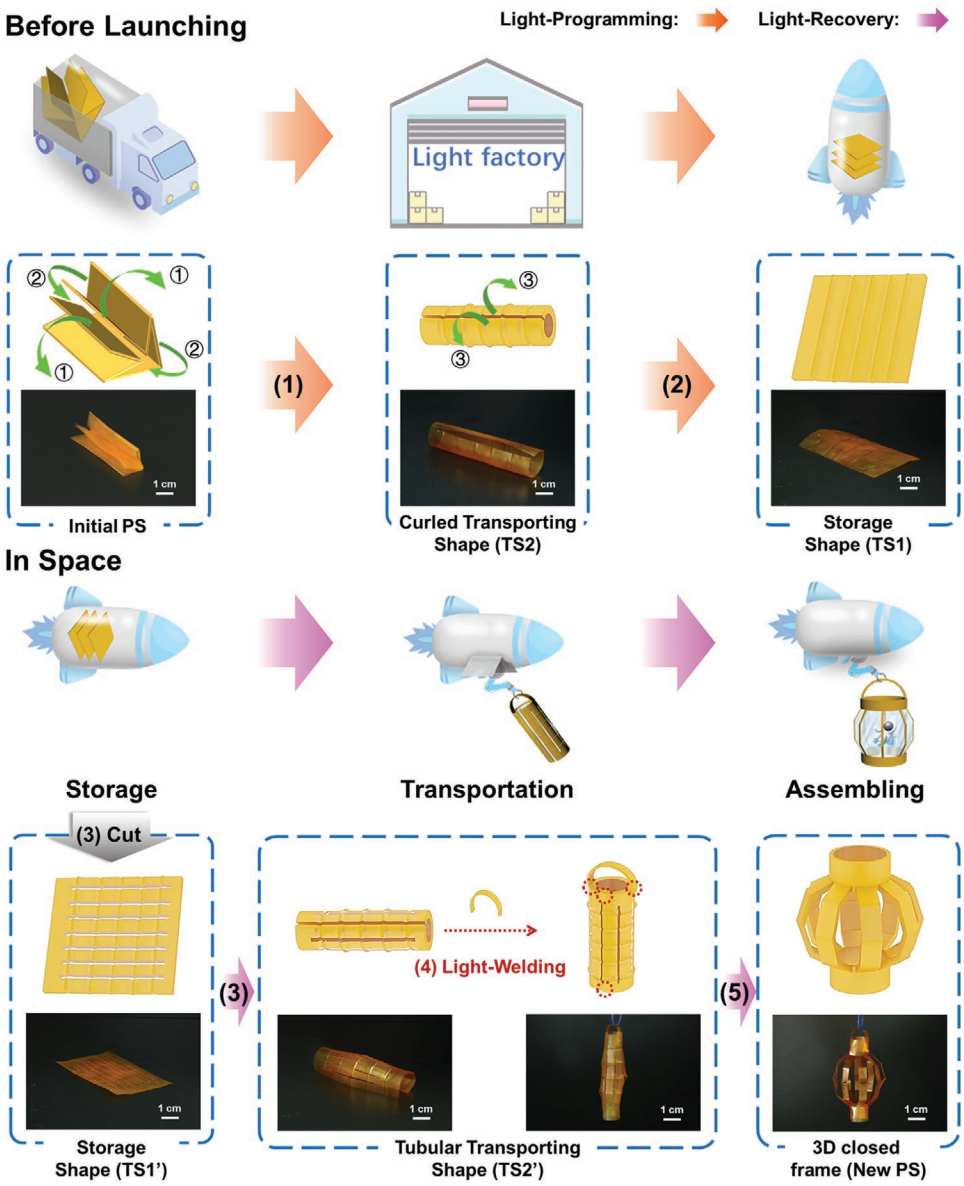

Figure 5. The photoorganizable operation for fabricating a kirigami 3D space capsule frame under light stimulation. The initial PS was first light-programmed into a curled TS2 under 150 mW cm^{-2} UV (365 nm) illumination (step 1). The programming was achieved by unfolding the film as indicated by green arrows ① and then rolling it along the direction as indicated by green arrows ②. After obtained the curled transporting shape (TS2), the UV light was removed and the film was flattened as indicated by green arrows ③ into a flat storage shape (TS1), followed by illumination of 530 visible light at 80 mW cm^{-2} (step 2). After TS1 was cut into TS1' according to the method shown in Figure S15 in the Supporting Information, 50 mW cm^{-2} UV light (365 nm) was shined to recover and roll up the sample for light-welding process (step 3). The sample was then light-welded with additional POTSMP stripe at PS into a tubular structure with a handle (TS2') by applying 500 mW cm^{-2}, 365 UV light to the red circle positions (step 4). Finally, through the localized light recovery using 150 mW cm^{-2} UV light (365 nm), the sample underwent recovery and produce a 3D closed frame as a new PS (step 5).

followed by cooling to room temperature to achieve a POTSMP thin film. The light reconfiguration, including light-reshaping process (locally deforming in one POTSMP sample) and light-welding process (local bonding of multiple POTSMP samples) could be realized according to the following operations.

Light-Reshaping Process: The POTSMP film was cut into desired shape and folded into 2D or 3D structures under 500 mW cm^{-2}, 365 nm UV irradiation for 10 s. After the removal of UV light, the permanent shape was cooled to room temperature and fixed before the removal of stress.

Light-Welding Process: One POTSMP film was first irradiated with 500 mW cm^{-2} UV light, and then immediately placed onto another POTSMP film to complete the preliminary welding. Subsequently, the cross-section of the welded point was irradiated by 500 mW cm^{-2} UV light until the two films were welded completely.

Light Programming of POTSMP: The sample was first illuminated under 150 mW cm^{-2}, 365 nm UV irradiation to program TS2. After the sample being processed into desired TS2, the UV light was turned off so that the material was cooled down to fix its TS2. As the sample stayed the rubbery state, it was then directly deformed into TS1 and was fixed by 80 mW cm^{-2}, 530 nm visible light irradiation for 3 min.

Light-Recovery Process of POTSMP: The localized light-recovery process from TS1 to TS2 of POTSMP was realized by shining 50 mW cm^{-2},

365 nm UV light at desired position for 300 s. The recovery of POTSMP from TS2 to PS was under the irradiation of 150 mW cm^{-2}, 365 nm UV light. The sample after each shape recovery could be irradiated by 80 mW cm^{-2}, 530 nm visible light for 3 min to recover POTSMP from *cis*-form to *trans*-form.

Supporting Information

Supporting Information is available from the Wiley Online Library or from the author.

Acknowledgements

This work was supported financially from the National Natural Science Foundation of China (51903054, 51927805), Natural Science Foundation of Shanghai (19ZR1404500), and "Chenguang Program" (18CG01) supported by Shanghai Education Development Foundation and Shanghai Municipal Education Commission.

Conflict of Interest

The authors declare no conflict of interest.

Data Availability Statement

The data that supports the findings of this study are available in the supplementary material of this article.

Keywords

azobenzene-containing polymers, light reconfiguration, photoorganizable performance, smart deployable structures, triple shape memory

Received: October 22, 2021
Revised: November 21, 2021
Published online:

[1] L. Puig, A. Barton, N. Rando, *Acta Astronaut.* **2010**, *67*, 12.
[2] E. A. Peraza-Hernandez, D. J. Hartl, R. J. Malak Jr, D. C. Lagoudas, *Smart Mater. Struct.* **2014**, *23*, 094001.
[3] Y. Liu, H. Du, L. Liu, J. Leng, *Smart Mater. Struct.* **2014**, *23*, 023001.
[4] B. Xu, C. Zhu, L. Qin, J. Wei, Y. Yu, *Small* **2019**, *15*, 1901847.
[5] J. Sun, Y. Wang, W. Liao, Z. Yang, *Small* **2021**, *17*, 2103700.
[6] H. Lu, B. Wu, X. Yang, J. Zhang, Y. Jian, H. Yan, D. Zhang, Q. Xue, T. Chen, *Small* **2020**, *16*, 2005461.
[7] J.-H. Choi, J. Ahn, J.-B. Kim, Y.-C. Kim, J.-Y. Lee, I.-K. Oh, *Small* **2016**, *12*, 1840.
[8] K. Oliver, A. Seddon, R. S. Trask, *J. Mater. Sci.* **2016**, *51*, 10663.
[9] Y. Xia, Y. He, F. Zhang, Y. Liu, J. Leng, *Adv. Mater.* **2021**, *33*, 2000713.
[10] R. Liang, H. Yu, L. Wang, N. Wang, B. U. Amin, *Adv. Funct. Mater.* **2021**, *31*, 2102621.
[11] A. Lendlein, O. E. C. Gould, *Nat. Rev. Mater.* **2019**, *4*, 116.
[12] Z. Cheng, D. Zhang, T. Lv, H. Lai, E. Zhang, H. Kang, Y. Wang, P. Liu, Y. Liu, Y. Du, S. Dou, L. Jiang, *Adv. Funct. Mater.* **2018**, *28*, 1705002.
[13] R. Liu, X. Kuang, J. Deng, Y.-C. Wang, A. C. Wang, W. Ding, Y.-C. Lai, J. Chen, P. Wang, Z. Lin, H. J. Qi, B. Sun, Z. L. Wang, *Adv. Mater.* **2018**, *30*, 1705195.
[14] M. Li, J. Chen, M. Shi, H. Zhang, P. X. Ma, B. Guo, *Chem. Eng. J.* **2019**, *375*, 121999.
[15] A. Lendlein, H. Jiang, O. Jünger, R. Langer, *Nature* **2005**, *434*, 879.
[16] T. Lv, Z. Cheng, E. Zhang, H. Kang, Y. Liu, L. Jiang, *Small* **2017**, *13*, 1503402.
[17] S.-Y. Leo, W. Zhang, Y. Zhang, Y. Ni, H. Jiang, C. Jones, P. Jiang, V. Basile, C. Taylor, *Small* **2018**, *14*, 1703515.
[18] I. Bellin, S. Kelch, R. Langer, A. Lendlein, *Proc. Natl. Acad. Sci. USA* **2006**, *103*, 18043.
[19] T. Xie, *Nature* **2010**, *464*, 267.
[20] S.-K. Ahn, R. M. Kasi, *Adv. Funct. Mater.* **2011**, *21*, 4543.
[21] X. Hu, D. Zhang, S. S. Sheiko, *Adv. Mater.* **2018**, *30*, 1707461.
[22] H. Jia, K. Chang, S.-Y. Gu, *Chin. J. Polym. Sci.* **2019**, *37*, 1119.
[23] K. M. Lee, H. Koerner, R. A. Vaia, T. J. Bunning, T. J. White, *Soft Matter* **2011**, *7*, 4318.
[24] X. Zhang, C. Zhu, B. Xu, L. Qin, J. Wei, Y. Yu, *ACS Appl. Mater. Interfaces* **2019**, *11*, 46212.
[25] H. Zhang, Y. Zhao, *ACS Appl. Mater. Interfaces* **2013**, *5*, 13069.
[26] B. T. Michal, C. A. Jaye, E. J. Spencer, S. J. Rowan, *ACS Macro Lett.* **2013**, *2*, 694.
[27] S. Ji, F. Fan, C. Sun, Y. Yu, H. Xu, *ACS Appl. Mater. Interfaces* **2017**, *9*, 33169.
[28] L. Yu, Q. Wang, J. Sun, C. Li, C. Zou, Z. He, Z. Wang, L. Zhou, L. Zhang, H. Yang, *J. Mater. Chem. A* **2015**, *3*, 13953.
[29] H. Xie, X. Y. Deng, C. Y. Cheng, K. K. Yang, Y. Z. Wang, *Macromol. Rapid Commun.* **2017**, *38*, 1600664.
[30] Y. Bai, J. Liu, J. Ju, X. Chen, *ACS Appl. Mater. Interfaces* **2021**, *13*, 23011.
[31] S. Fu, H. Zhang, Y. Zhao, *J. Mater. Chem. C* **2016**, *4*, 4946.
[32] Y. Li, O. Rios, J. K. Keum, J. Chen, M. R. Kessler, *ACS Appl. Mater. Interfaces* **2016**, *8*, 15750.
[33] L. Zhou, Q. Liu, X. Lv, L. Gao, S. Fang, H. Yu, *J. Mater. Chem. C* **2016**, *4*, 9993.
[34] Z.-B. Wen, D. Liu, X.-Y. Li, C.-H. Zhu, R.-F. Shao, R. Visvanathan, N. A. Clark, K.-K. Yang, Y.-Z. Wang, *ACS Appl. Mater. Interfaces* **2017**, *9*, 24947.
[35] D. Habault, H. Zhang, Y. Zhao, *Chem. Soc. Rev.* **2013**, *42*, 7244.
[36] Z. Fang, H. Song, Y. Zhang, B. Jin, J. Wu, Q. Zhao, T. Xie, *Matter* **2020**, *2*, 1187.
[37] W. Miao, W. Zou, B. Jin, C. Ni, N. Zheng, Q. Zhao, T. Xie, *Nat. Commun.* **2020**, *11*, 4257.
[38] B. Zhang, H. Li, J. Cheng, H. Ye, A. H. Sakhaei, C. Yuan, P. Rao, Y.-F. Zhang, Z. Chen, R. Wang, X. He, J. Liu, R. Xiao, S. Qu, Q. Ge, *Adv. Mater.* **2021**, *33*, 2101298.
[39] B. Jin, H. Song, R. Jiang, J. Song, Q. Zhao, T. Xie, *Sci. Adv.* **2018**, *4*, eaao3865.
[40] H. Zhang, D. Wang, N. Wu, C. Li, C. Zhu, N. Zhao, J. Xu, *ACS Appl. Mater. Interfaces* **2020**, *12*, 9833.
[41] F. Song, Z. Li, P. Jia, M. Zhang, C. Bo, G. Feng, L. Hu, Y. Zhou, *J. Mater. Chem. A* **2019**, *7*, 13400.
[42] Y. Jin, Z. Lei, P. Taynton, S. Huang, W. Zhang, *Matter* **2019**, *1*, 1456.
[43] H. Zhou, C. Xue, P. Weis, Y. Suzuki, S. Huang, K. Koynov, G. K. Auernhammer, R. Berger, H.-J. Butt, S. Wu, *Nat. Chem.* **2017**, *9*, 145.
[44] Q. Liu, Y. Liu, J.-A. Lv, E. Chen, Y. Yu, *Adv. Intell. Syst.* **2019**, *1*, 1900060.
[45] W.-C. Xu, S. Sun, S. Wu, *Angew. Chem., Int. Ed.* **2019**, *58*, 9712.
[46] W. Peng, G. Zhang, J. Liu, S. Nie, Y. Wu, S. Deng, G. Fang, J. Zhou, J. Song, J. Qian, P. Pan, Q. Zhao, T. Xie, *Adv. Funct. Mater.* **2020**, *30*, 2000522.
[47] Y. Song, Y. Liu, T. Qi, G. L. Li, *Angew. Chem., Int. Ed.* **2018**, *57*, 13838.
[48] J. Leng, X. Wu, Y. Liu, *J. Appl. Polym. Sci.* **2009**, *114*, 2455.